Publication Year	2015
Acceptance in OA	2020-04-10T13:00:17Z
Title	Spectroscopic response and charge transport properties of CdZnTe detectors grown by the vertical Bridgman technique
Authors	Abbene, L., Gerardi, G., Turturici, A. A., Raso, G., DEL SORDO, STEFANO, CAROLI, EZIO, AURICCHIO, NATALIA, Benassi, G., Zambelli, N., Zappettini, A., Principato, F.
Publisher's version (DOI)	10.1109/NSSMIC.2015.7582269
Handle	http://hdl.handle.net/20.500.12386/23987
Serie	PROCEEDINGS..IEEE NUCLEAR SCIENCE SYMPOSIUM AND MEDICAL IMAGING CONFERENCE

Spectroscopic Response and Charge Transport Properties of CdZnTe Detectors Grown by the Vertical Bridgman Technique

L. Abbene*, G. Gerardi, A. A. Turturici, G. Raso, S. Del Sordo, E. Caroli, N. Auricchio, G. Benassi, N. Zambelli, A. Zappettini and F. Principato

***Abstract*–In this work, we present the results of spectroscopic investigations on CdZnTe (CZT) detectors grown by the boron oxide encapsulated vertical Bridgman technique (IMEM-CNR, Parma, Italy). The detectors, with different thicknesses (1 and 2.5 mm), are characterized by the same electrode layout (gold electroless contacts): the anode is a central electrode (2 x 2 mm^2) surrounded by a guard-ring electrode, while the cathode is a planar electrode covering the detector surface (4.1 x 4.1 mm^2). The results of electrical investigations point out the low leakage currents of these detectors even at high bias voltages: 38 nA/cm^2 (T = 25°C) at 10000 V/cm. The time-stability and the spectroscopic response of the detectors, at different temperatures and fluxes, were investigated. ^{241}Am spectra were measured up to 1 Mcps. The detectors were compared with the traveling heater method (THM) CZT grown detectors (Redlen), fabricated with the same electrode layout. These activities are in the framework of an Italian research project on the development of energy-resolved photon counting (ERPC) systems for high flux energy-resolved X-ray imaging.**

I. Introduction

In the last two decades, cadmium telluride (CdTe) and cadmium zinc telluride (CdZnTe or CZT) detectors have been widely developed and used for room temperature X-ray and gamma ray spectroscopy [1-3]. CZT/CdTe detectors with thicknesses of 2–3 mm are able to effectively absorb X rays in the 1–150 keV range and to provide good energy resolution even at room temperature. Recently, CdTe/CZT detectors with pixelated electrode structures, are also proposed for the development of energy-resolved photon counting (ERPC) systems for high flux energy-resolved X-ray imaging, very appealing in diagnostic medicine, industrial imaging and security screening [4-9]. Due to the high-flux conditions of these applications ($>10^6$ photons mm^{-2} s^{-1}), detectors with high bias voltage operation and optimum charge collection are required. CZT detectors with quasi-ohmic contacts (Au/CZT/Au, Pt/CZT/Pt) [6,10,11] compete with CdTe detectors with rectifying contacts (In/CdTe/Pt, Al/CdTe/Pt) [1,7,9,12], taking into account low-rate [13-16] and high-rate polarization phenomena [17-18].

Recently, within an Italian research collaboration (University of Palermo, IMEM-CNR Parma, IASF/INAF Bologna and Palermo), we proposed to develop ERPC prototypes, based on CZT detectors and digital pulse processing (DPP) electronics, for high flux energy resolved X-ray imaging applications (1-140 keV). In the framework of these activities, we developed, at first step, some CZT prototypes, with planar electrode structures, to investigate on both the crystal and the device properties. In this work, we will present the results of spectroscopic investigations (X-ray response at both low and high fluxes, charge transport properties, temperature dependence and spectral improvements through digital pulse height and shape analysis) on boron oxide encapsulated vertical Bridgman grown CZT detectors, recently developed at IMEM-CNR Parma, Italy [2, 19-25].

A comparison with the traveling heater method (THM) CZT grown detectors (REDLEN, Canada), fabricated with the same electrode layout (gold electroless contacts by IMEM-CNR Parma, Italy), was also presented.

II. Detectors and Operation

The detectors are based on CZT crystals (4.1 x 4.1 x 1, 2.5 mm^3), grown by the boron oxide encapsulated vertical Bridgman (B-VB) technique, which are currently produced at IMEM-CNR (Parma, Italy) [2, 19-25]. Some detector samples are based on traveling heater method (THM) CZT grown crystals (4.1 x 4.1 x 1, 3 mm^3), produced by Redlen Techonologies Inc. (Canada) [10, 11, 26]. Gold electroless contacts were realized on both the anode (prepared by using water solutions) and the cathode (prepared by alcoholic solutions) of the CZT samples. The anode surface is characterized, for all detectors, by a central electrode (2 x 2 mm^2) surrounded by a guard-ring electrode (Fig. 1). The width of the guard-ring is 950 μm and the gap between the electrodes is 50 μm. The cathode is a planar electrode

Manuscript received December,,,,,. This work was supported by the Italian Ministry for Education, University and Research (MIUR) under PRIN Project No. 2012WM9MEP.

Leonardo Abbene is with Dipartimento di Fisica e Chimica, Università di Palermo, Viale delle Scienze, Edificio 18, Palermo 90128, Italy (corresponding author, telephone 0039-091-23899081, e-mail: leonardo.abbene@unipa.it).

G. Gerardi, F. Principato, A. A. Turturici and G. Raso are with Dipartimento di Fisica e Chimica, Università di Palermo, Viale delle Scienze, Edificio 18, Palermo 90128, Italy.

A. Zappettini is with IMEM/CNR, Parco Area delle Scienze 37/A, 43100 Parma, Italy.

G. Benassi and N. Zambelli are with due2lab s.r.l., Viale Mariotti 1, Parma, Italy.

N. Auricchio, E. Caroli and S. Del Sordo are with IASF/INAF Bologna and Palermo, Italy.

covering the detector surface. The main characteristics of the samples are summarized in Table I.

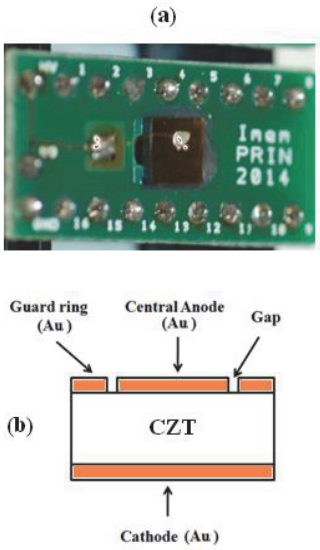

Fig. 1. (a) The 1 mm thick CZT detector (cathode side view). (b) Schematic cross section view of the detectors.

TABLE I. CHARACTERISTICS OF THE SAMPLES

Sample	Crystal Size (mm^3)	Growth Technique	Electrodes
IMEM 2	4.1 x 4.1 x 1	B-VB	Gold (Electroless)
REDLEN 2.1	4.1 x 4.1 x 1	THM	Gold (Electroless)
IMEM 2.2	4.1x 4.1 x 2.5	B-VB	Gold (Electroless)
REDLEN 2	4.1 x 4.1 x 3	THM	Gold (Electroless)

The electrical properties (current-voltage curves) of the detectors were measured by using a high voltage source meter Keithley 2410, which provides the detector bias voltage, and the source-measure unit Keithley 236 configured as electrometer. The guard ring of the detectors is held at zero potential to prevent surface leakage currents.

The spectroscopic characterization of the detectors, at low photon counting rates (ICRs), was performed by using a standard analog electronics. To amplify and filter the detector signals, we used a commercial AC-coupled charge sensitive preamplifier CSP (A250, Amptek, USA; nominal ENC of about 1 keV) and a standard spectroscopy amplifier (672, ORTEC, USA), equipped with different shaping time constant values of 0.5, 1, 2, 3, 6, and 10 μs. A commercial multichannel analyzer (MCA-8000A, Amptek, USA) was used to sample and to record the shaped signals.

To measure the spectroscopic response of the detectors at high ICRs, we used a digital pulse processing (DPP) electronics, recently developed by our group [27-30]. The DPP system, based on direct digitizing and processing of the preamplifier output signals, is able to perform a fine pulse shape and height analysis (PSHA) on the pulses selected through a pile-up rejection (PUR). All detector pulses (i.e. preamplifier output pulses) are analyzed within a time window (*Snapshot*) with a time width termed *Snapshot Time* (*ST*). The *ST* values strongly affect the energy resolution as the shaping time constant of the analog electronics. The digital system is also able to apply the pulse shape discrimination (PSD) technique to minimize both incomplete charge collection and pile-up [31-34].

Both the detectors and the CSP were enclosed in a shielded box placed on a Peltier thermal stage with temperature control within 0.1°C, and filled with nitrogen gas to prevent condensation.

III. ELECTRICAL AND CHARGE TRANSPORT PROPERTIES

Fig. 2 shows the current-voltage (*I-V*) characteristics of the 1 mm thick sample (IMEM2) at room temperature (T = 25 °C) and at T = 15 °C. The behaviour of the I-V curves is typical of the Au/CZT/Au contacts, i.e. of a metal–semiconductor–metal (MSM) device with two back-to-back Schottky barriers [35]. As clearly visible in the figure, the detector is characterized by very low leakage currents in the reverse bias region: 3.5 nA/cm^2 at 1000 V/cm at T = 25 °C (1.2 nA/cm^2 at T = 15°C); typically, Au/CZT/Au detectors (fabricated by Redlen) are characterized by leakage currents ranging from 50 nA/cm^2 to

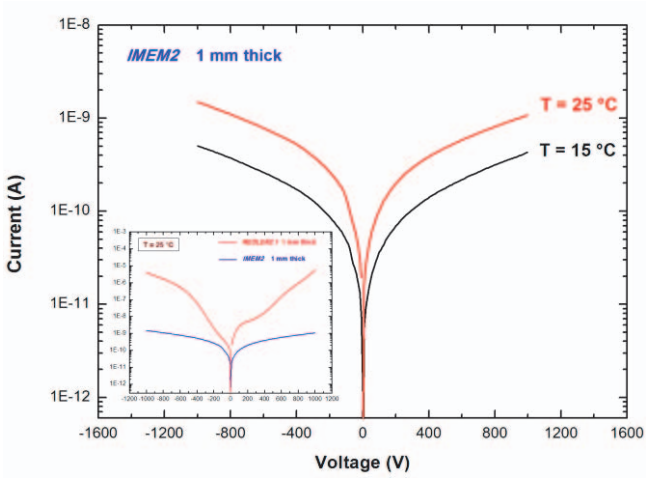

Fig. 2. The current-voltage characteristics of the 1 mm thick CZT detector at (IMEM2) room temperature (T=25 °C) and at T = 15°C. The inset also shows the current-voltage curves of both IMEM2 and REDLEN2.1 (1 mm thick) at room temperature.

500 nA/cm^2 at 1000 V/cm [10-11]. Moreover, low leakage current of 38 nA/cm^2 (T = 25°C) characterizes the IMEM2 detector at very high electric field of 10000 V/cm.

The inset of Fig.2 also shows the *I-V* curve of the 1 mm thick REDLEN2.1 sample, with leakage current values (13 nA/cm^2 at 1000 V/cm) in agreement with the literature (from 50 nA/cm^2 to 500 nA/cm^2 at 1000 V/cm) [10-11]. Despite the samples were fabricated with the same electrode technique, the REDLEN2.1 sample is characterized by higher leakage

currents than the IMEM2 one. This difference is due to the different barrier heights of detectors [36]: 1.1 e V for IMEM and 0.9 eV for REDLEN [36]. All samples are characterized by similar resistivity values (~2x10^{10} Ω·cm) [36]. Probably, the differences in the barrier height between IMEM and REDLEN detectors are due to the different crystal orientation [37].

To characterize the charge transport properties of the detectors, we also measured the mobility-lifetime product of the electrons $\mu_e\tau_e$. To evaluate the $\mu_e\tau_e$, we irradiated the detector from the cathode side, by using the 22.1 keV line of the ^{109}Cd source, and the energy spectra at different bias voltages were measured. The charge collection efficiencies at 22.1 keV vs. the bias voltage are reported in Fig. 3. The experimental points are fitted with the simplified Hecht equation [38]. This result points out as the IMEM detectors are characterized by lower charge transport properties ($\mu_e\tau_e$) than the REDLEN ones.

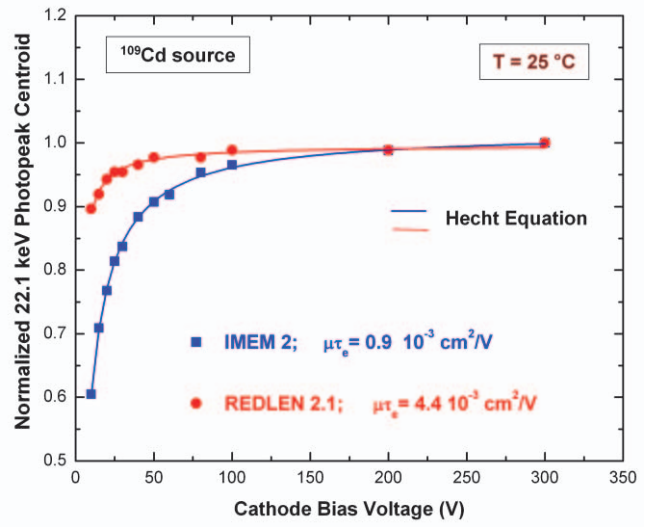

Fig. 3. The normalized 22.1 keV photopeak centroid (i.e. the charge collection efficiency) at various cathode bias voltages for IMEM2 and REDLEN2.1 detectors. The experimental points are fitted with the simplified Hecht equation [38]. The analog electronics with a shaping time constant of 2 us was used.

IV. Spectroscopic Response of the Detectors

A. Response at low photon counting rates

The time-stability of the detectors, within a time window of 40 minutes, at different temperatures (T = 25, 15, 5, 0, -5, −15 °C) was first investigated. Generally, all detectors showed good time-stability at all temperatures, in agreement with the literature [2]. Fig. 4 shows the time evolution of the spectroscopic response of IMEM2 detector (^{241}Am source) at T = -5 °C (bias voltage equal to -200 V).

Fig. 5 shows the energy resolution (FWHM at 59.5 keV) vs. the bias voltage of the IMEM2 detector at different temperatures. At room temperature, the optimum energy resolution (4.6%) was obtained at 6000 V/cm, while an energy resolution of 5.4 % was obtained at 10000 V/cm. At temperatures below 5 °C, no performance improvements were observed. Generally, similar low-rate performance for all detectors were measured (^{241}Am source), but obtained at different optimum bias voltages. Fig. 6 shows a comparison

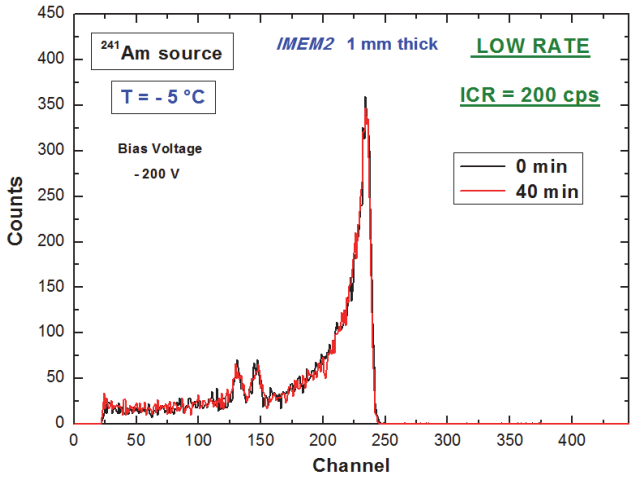

Fig. 4. The measured ^{241}Am spectra (ICR = 200 cps) of the IMEM2 detector, just after biasing (black line) and after 40 minutes (red line). The analog electronics with a shaping time constant of 1 μs was used.

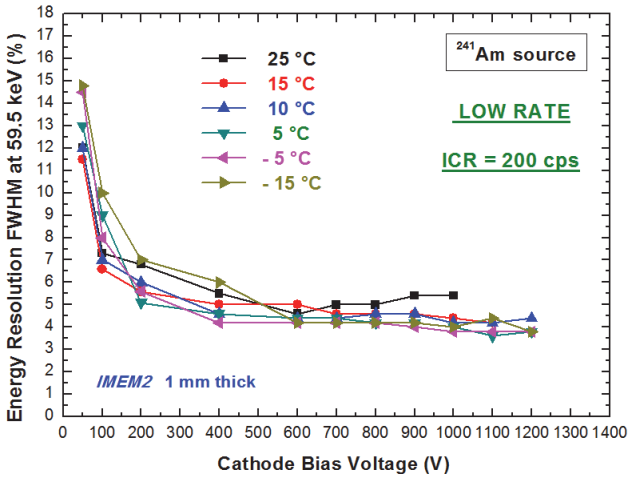

Fig. 5. Energy resolution (FWHM) at 59.5 keV vs. the bias voltage at different temperatures for the IMEM2 detector. The analog electronics with a shaping time constant of 1 μs was used.

between the performance of IMEM2 and REDLEN2.1 at room temperature. Both detectors are characterized by similar room temperature performance, but obtained at different bias voltages. The optimum bias voltage, for the REDLEN2.1, is at 2000 V/cm, in agreement with the literature. The IMEM2 detector, in agreement with the I-V curves, allows high bias voltage operation, very important for high-rate measurements. The low-rate performance (59.5 and 122.1 keV) of IMEM detectors are reported in Table II. The ^{241}Am and ^{57}Co spectra measured with the IMEM2 detector at T = 5 °C are shown in Figs. 7 and 8.

B. Response at high photon counting rates

The time-stability at high ICRs was investigated (within a time window of 30 minutes). Fig. 9 shows the time stability of the spectroscopic response of IMEM2 detector (^{241}Am source) at ICR = 660 kcps (bias voltage of 1000 V and electric field of 10000 V/cm).

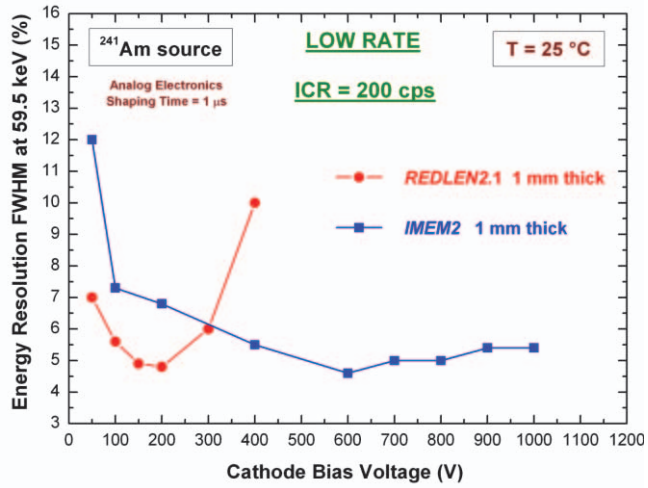

Fig. 6. Energy resolution (FWHM) at 59.5 keV vs. the bias voltage at room temperature for the IMEM2 and REDLEN2.1 detectors. The analog electronics with a shaping time constant of 1 µs was used.

TABLE I. LOW-RATE SPECTROSCOPIC PERFORMANCE OF THE IMEM SAMPLES

Sample and Optimum Field Strength	T (°C)	Energy Resolution at 59.5 keV (%)	Energy Resolution at 122.1 keV (%)
IMEM 2 -6000 V/cm	25	4.6	4.6
IMEM 2 -11000 V/cm	5	3.6	3.4
IMEM 2.2 -4000 V/cm	25	4.5	4
IMEM 2.2 -7200 V/cm	5	3.7	3.5

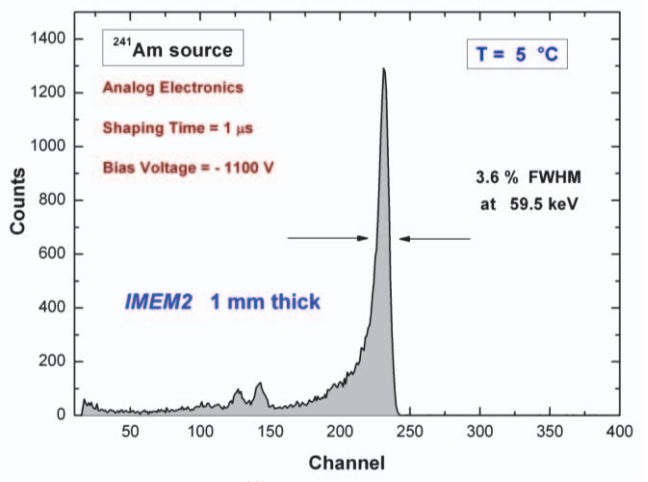

Fig 7. The measured ^{241}Am spectrum for the IMEM2 detector.

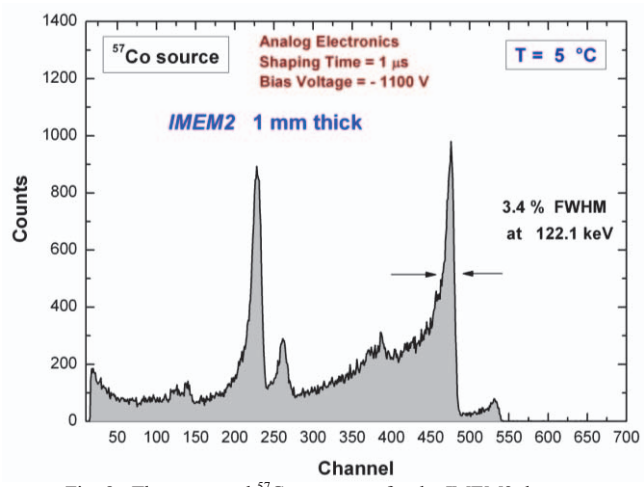

Fig. 8. The measured ^{57}Co spectrum for the IMEM2 detector.

The time-stability of the IMEM2.2 was also verified at ICR = 1 Mcps (bias voltage of 1800 V and electric field of 7200 V/cm). Fig. 10 shows the measured ^{241}Am spectra with the IMEM2 detector at different bias voltages. The energy resolution (FWHM at 59.5 keV) vs. the bias voltage of the IMEM2 and REDLEN2.1 detectors is reported in Fig. 11. At high rates, higher bias voltages are required, if compared with the low-rate condition.

Fig. 12 shows the measured ^{241}Am spectra with both REDLEN2 (3 mm thick) and IMEM2.2 (2.5 mm thick) at 1 Mcps. The best ^{241}Am spectra measured with the two IMEM detectors, after PUR and PSD, are shown in Figs. 13 and 14.

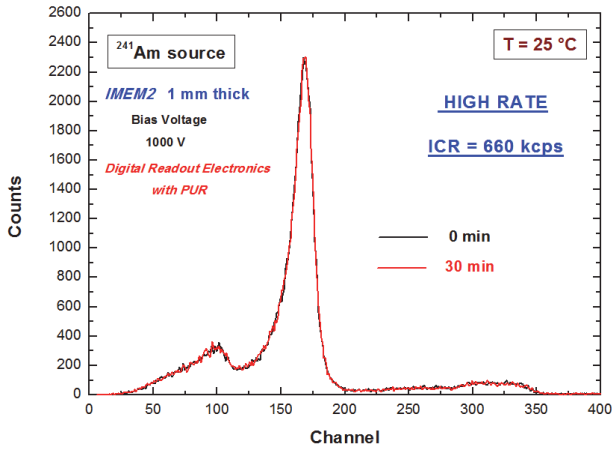

Fig. 9. The measured ^{241}Am spectra (ICR = 660 kcps) of the IMEM2 detector, just after biasing (black line) and after 30 minutes (red line). The digital electronic with a *ST* = 5µs, equipped with a pile-up rejection (PUR) was used.

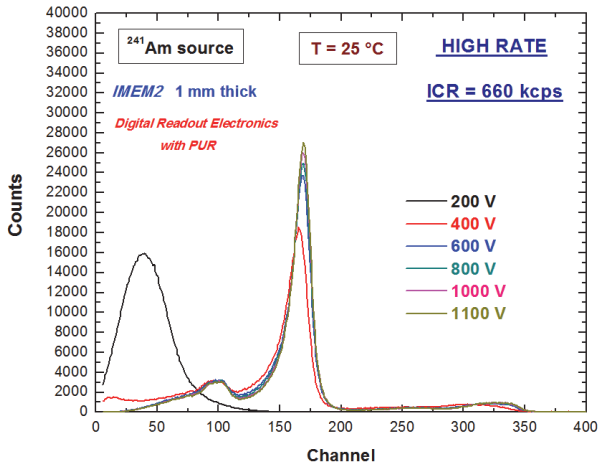

Fig. 10. The measured ^{241}Am spectra (ICR = 660 kcps) of the IMEM2 detector at different cathode bias voltages. The digital electronic with a *ST* = 5µs, equipped with a pile-up rejection (PUR) was used.

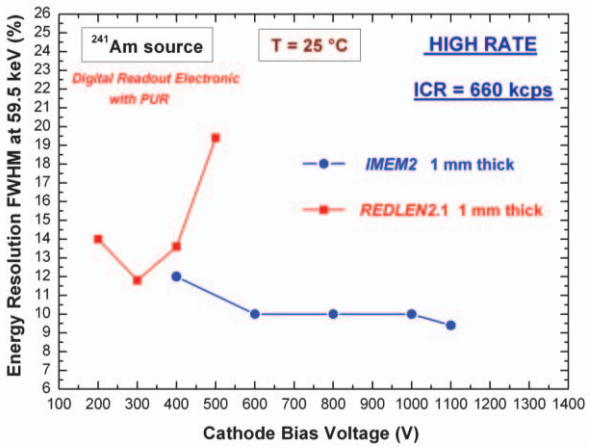

Fig. 11. Energy resolution (FWHM) at 59.5 keV vs. the bias voltage at room temperature for the IMEM2 and REDLEN2.1 detectors. The digital electronic with a *ST* = 5µs, equipped with a pile-up rejection (PUR) was used.

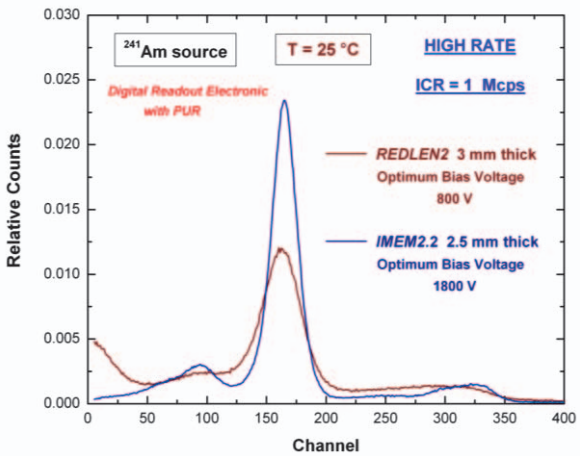

Fig. 12. The measured ^{241}Am spectra (ICR = 1Mcps) of the IMEM2.2 and REDLEN2 detectors. The digital electronic with a *ST* = 4µs, equipped with a pile-up rejection (PUR) was used.

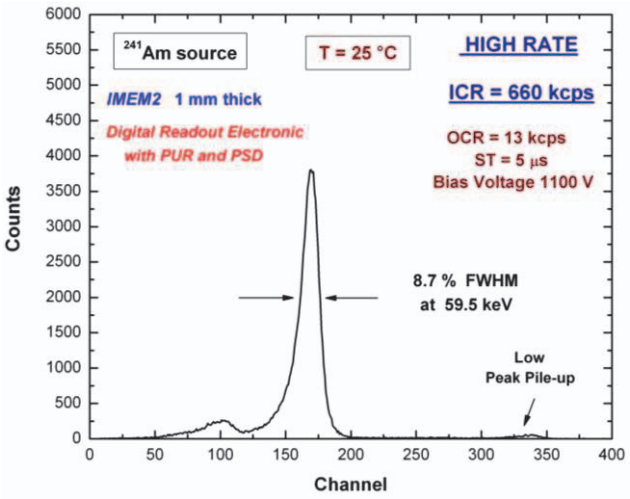

Fig. 13. The measured ^{241}Am spectrum (ICR = 660 kcps) of the IMEM2 detector, after digital PUR (pile-up rejection) and PSD (pulse shape discrimination).

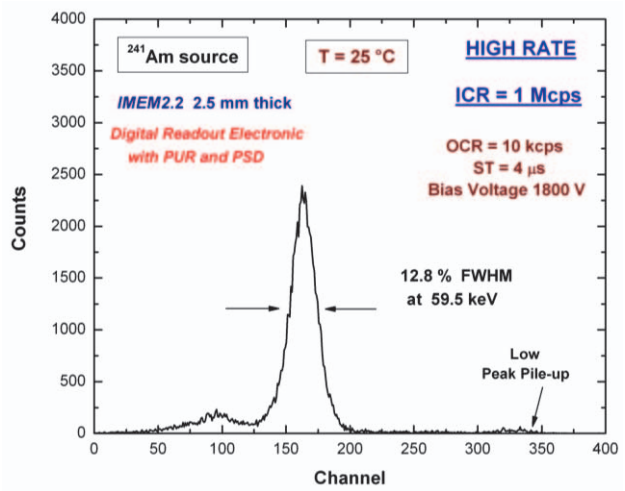

Fig. 14. The measured ^{241}Am spectrum (ICR = 1 Mcps) of the IMEM2.2 detector, after digital PUR (pile-up rejection) and PSD (pulse shape discrimination).

V. Conclusions

The spectroscopic response of planar CZT detectors (IMEM detectors) grown by the boron oxide encapsulated vertical Bridgman (B-VB) technique was investigated at both low and high photon counting rates. The main results are summarized below:

(i) the IMEM detectors (Au/CZT/Au) are characterized by very low leakage currents even at high bias voltages: 3.5 nA/cm^2 at 1000 V/cm and 38 nA/cm^2 at 10000 V/cm at room temperature;

(ii) the measured mobility-lifetime product of the electrons $\mu_e\tau_e$ is equal to 10^{-3} cm^2/V;

(iii) at low rates, the time-stability of the detectors, within a time window of 40 minutes, at different temperatures (T = 25, 15, 5, 0, -5, −15 °C) was verified. The spectroscopic performance of the detectors are similar to some REDLEN CZT detectors (grown by the traveling heater method) fabricated with the same electrode layout;

(iv) at high rates (up to 1 Mcps), the time-stability of the detectors at room temperature, within a time window of 30 minutes, was verified; in these conditions, the high-rate performance of the detectors are better than the REDLEN ones, due to the possibility to operate at very high bias voltages without an excessive increase of the noise due to the leakage currents.

ACKNOWLEDGMENT

This work was supported by the Italian Ministry for Education, University and Research (MIUR) under PRIN Project No. 2012WM9MEP.

REFERENCES

[1] T. Takahashi and S. Watanabe, "Recent progress in CdTe and CdZnTe detectors," IEEE Trans. Nucl. Sci., vol. 48, no. 4, pp. 950-959, 2001.

[2] S. Del Sordo et al., "Progress in the development of CdTe and CdZnTe semiconductor radiation detectors for astrophysical and medical applications," Sensors , vol. 9, pp. 3491-3526, 2009.

[3] L. Abbene and S. Del Sordo, "CdTe Detectors," in Comprehensive Biomedical Physics, vol. VIII, A. Brahme ed. Elsevier, 2014, pp. 285-314.

[4] K. Taguchi et al., "Vision 20/20: Single photon counting x-ray detectors in medical imaging," Med. Phys., vol. 40, 100901, 2013.

[5] E. Fredenberg et al., "Energy resolution of a photon-counting silicon strip detector," Nucl. Instr. and Meth., vol. A 613, pp. 156-162, 2010.

[6] J. S. Iwanczyk et al., "Photon Counting Energy Dispersive Detector Arrays for X-ray Imaging," IEEE Trans. Nucl. Sci., vol. 56, no. 3, pp. 535-542, 2009.

[7] K. Ogawa et al., "Development of an energy-binned photon-counting detector for X-ray and gamma-ray imaging," Nucl. Instr. and Meth., vol. A 664, pp. 29-37, 2012

[8] A. Brambilla et al., "Fast CdTe and CdZnTe semiconductor detector arrays for spectroscopic x-ray imaging," IEEE Trans. Nucl. Sci., vol. 60, no. 1, pp. 408-415, 2013.

[9] L. Abbene et al., "Digital performance improvements of a CdTe pixel detector for high flux energy-resolved X-ray imaging," Nucl. Instr. and Meth., vol. A 777, pp. 54-62, 2015.

[10] H. Chen et al., " Characterization of Traveling Heater Method (THM) Grown Cd0.9Zn0.1Te Crystals" IEEE Trans. Nucl. Sci., vol. 54, no. 4, pp. 811-816, 2007.

[11] S. A. Awadalla et al., "High voltage optimization in CdZnTe detectors," Nucl. Instr. and Meth., vol. A 764, pp. 193-197, 2014.

[12] L. Abbene et al., "Experimental results from Al/p-CdTe/Pt X-ray detectors," Nucl. Instr. and Meth., vol. A 730, pp. 135-140, 2013.

[13] I. Farella et al.," Study on Instability Phenomena in CdTe Diode-Like Detectors," *IEEE Trans. Nucl. Sci.*, vol. 56, no. 4, pp. 1736-1742, 2009.

[14] F. Principato et al., "Time-dependent current-voltage characteristics of Al/p-CdTe/Pt x-ray detectors," J. Appl. Phys., vol 112, 094506, 2012.

[15] A. A. Turturici et al., "Electrical characterization of CdTe pixel detectors with Al Schottky anode," Nucl. Instr. and Meth., vol. A 763, pp. 476-482, 2014.

[16] F. Principato et al., "Polarization phenomena in Al/p-CdTe/Pt X-ray detectors," Nucl. Instr. and Meth., vol. A 730, pp. 141-145, 2013.

[17] D. S. Bale et al.," Nature of polarization in wide-bandgap semiconductor detectors under high-flux irradiation: Application to semi-insulating Cd1−xZnxTe," PHYSICAL REVIEW B vol. 77, art. no. 035205, 2008.

[18] P. J. Sellin et al.," Electric field distributions in CdZnTe due to reduced temperature and x-ray irradiation," APPLIED PHYSICS LETTERS vol. 96, art. no. 133509, 2010.

[19] A. Zappettini et al., "Boron Oxide Encapsulated Vertical Bridgman Grown CdZnTe Crystals as X-Ray Detector Material, " IEEE Trans. Nucl. Sci., vol. 56, no. 4, pp. 1743-1746, 2009.

[20] A. Zappettini et al.,"Growth and characterization of CZT crystals by the Vertical Bridgman method for X-ray detector applications", IEEE Trans. Nucl. Sci., vol. 58, no. 5, pp. 2352-2356, 2011.

[21] A. Zappettini et al., "Boron Oxide Encapsulated Vertical Bridgman: A Method for Preventing Crystal-Crucible Contact in the CdZnTe Growth," IEEE Trans. Nucl. Sci., vol. 54, no. 4, pp. 798-801, 2007.

[22] A. Zappettini, M. Zha, M. Pavesi, L. Zanotti, "Boron oxide fully encapsulated CdZnTe crystals grown by the vertical bridgman tecnique, " J. Crystal Growth, vol. 307, no. 2, pp. 283–288, Sep. 2007.

[23] M. Zha, A. Zappettini, D. Calestani, L. Marchini, L. Zanotti, C. Paorici, "Full-encapsulated CdZnTe crystals by the vertical Bridgman method, " J. Crystal Growth, vol. 310, no. 7-9, pp. 2072–2075, 2008.

[24] N. Zambelli, L. Marchini, G. Benassi, D. Calestani, E. Caroli, A. Zappettini, "Electroless gold contact deposition on CdZnTe detectors by scanning pipette technique, " JINST 7, P08022, 2012.

[25] N. Auricchio et al., "Charge transport properties in CdZnTe detectors grown by the vertical Bridgman technique," J. Appl. Phys., vol. 110, art. no. 124502, 2011.

[26] H. Chen, S. A. Awadalla, K. Iniewski, P. H. Lu, F. Harris, J. MacKenzie, T. Hasanen, W. Chen, R. Redden, G. Bindley, I. Kuvvetli, C. Budtz-Jørgensen, P. Luke, M. Amman, J. S. Lee, A. E. Bolotnikov, G. S. Camarda, Y. Cui, A. Hossain, R. B. James, "Characterization of large cadmium zinc telluride crystals grown by traveling heater method, " J. Appl. Phys, vol. 103, art. no. 014903, 2008.

[27] L. Abbene et al., "Real time digital pulse processing for X-ray and gamma ray semiconductor detectors," Nucl. Instr. and Meth., vol. A 730, pp. 124-128, 2013.

[28] L. Abbene et al., "Energy resolution and throughput of a new real time digital pulse processing system for x-ray and gamma ray semiconductor detectors, " JINST, vol. 8, P07019, 2013.

[29] G. Gerardi, L. Abbene, "A digital approach for real time high-rate high-resolution radiation measurements," Nucl. Instr. and Meth., vol. A 768, pp. 46-54, 2014.

[30] L. Abbene and G. Gerardi, "High-rate dead-time corrections in a general purpose digital pulse processing system, " J. Synchrotron Rad. vol. 22, pp. 1190-1201, 2015.

[31] L. Abbene and G. Gerardi, "Performance enhancements of compound semiconductor radiation detectors using digital pulse processing techniques, " Nucl. Instr. and Meth., vol. A 654, pp. 340-348, 2011.

[32] L. Abbene, G. Gerardi, F. Principato, S. Del Sordo, R. Ienzi and G. Raso, "High-rate x-ray spectroscopy in mammography with a CdTe detector: a digital pulse processing approach," Med. Phys., vol. 37, pp. 6147-6156, 2010.

[33] L. Abbene, G. Gerardi, S. Del Sordo, G. Raso, "Performance of a digital CdTe X-ray spectrometer in low and high counting rate environment," Nucl. Instr. and Meth., vol. A 621, pp. 447-452, 2010.

[34] L. Abbene, G. Gerardi, F. Principato, S. Del Sordo, G. Raso, "Direct measurement of mammographic x-ray spectra with a digital CdTe detection system," Sensors , vol. 12, pp. 8390-8404, 2012.

[35] A. E. Bolotnikov, S. E. Boggs, C. M. Hubert Chen, W. R. Cook, F. A. Harrison, S. M. Schindler, "Properties of Pt Schottky type contacts on high-resistivity CdZnTe detectors, " Nucl. Instr. and Meth. A, vol. 481, pp. 395-407, 2002.

[36] A. A. Turturici et. al, "Charge Carrier Transport Mechanisms in CdZnTe Detectors Grown by the Vertical Bridgman Technique" *IEEE Nuclear Science Symposium Conference Record*, 2015, in press.

[37] S. J. Bell, M. A. Baker, D. D. Duarte, A. Schneider, P. Seller, P. J. Sellin, M. C. Veale, M. D. Wilson, "Characterization of the metal-semiconductor interface of gold contacts on CdZnTe formed by electroless deposition, " J. Phys. D: Appl. Phys, vol. 48 no. 27, art. no. 275304, 2015.

[38] P. J. Sellin et al., " Drift Mobility and Mobility-Lifetime Products in CdTe:Cl Grown by the Travelling Heater Method" IEEE Trans. Nucl. Sci., vol. 52, no. 6, pp. 3074-3078, 2005.